engineering proceedings

MDPI

Proceeding Paper

Experimental Analysis of Single-Slope Solar Still Equipped with Jute and Nano-Enhanced Jute Cloth for Clean Water Production †

Ravishankar Sathyamurthy [1,2]

[1] Department of Mechanical Engineering, King Fahd University of Petroleum & Minerals, Dhahran 31261, Saudi Arabia; r.sathyamurthy@kfupm.edu.sa
[2] IRC Sustainable Energy Systems, King Fahd University of Petroleum & Minerals, Dhahran 31261, Saudi Arabia

† Presented at the 1st International Online Conference on Inventions—Energy Security and Sustainable Development, 25–26 June 2026; Available online: https://sciforum.net/event/IOCIV2026.

Abstract

The global scarcity of potable water necessitates the development of efficient and low-cost desalination technologies. This study presents an experimental investigation into enhancing the productivity of a conventional single-slope solar still (SSSS) by employing natural jute cloth and nano-enhanced jute cloth as novel wick materials. The primary objective was to compare the performance of the modified stills with that of a conventional still under identical climatic conditions. The jute cloth was dip-coated with carbon black nanoparticles and a polyvinyl alcohol (PVA) binder to create a nano-enhanced wick with higher solar absorptivity. Three identical solar stills were fabricated and tested simultaneously on a representative clear-sky day: a conventional still (CSS), a still with jute cloth (JSS), and a still with nano-enhanced jute cloth (NJSS). Key performance parameters, including daily water yield, internal heat and mass transfer, and thermal efficiency, were meticulously measured and analysed. The experimental results demonstrated a significant improvement in productivity for the modified stills. The cumulative daily water yield for the CSS was 2.1 L/m^2. The JSS showed a marginal increase, producing 3.0 L/m^2, an improvement of about 43%. The NJSS outperformed both, achieving a yield of 3.8 L/m^2, which was relatively higher by about 81% compared to the conventional case. The efficiency of the CSS was 34%, increasing to 42% for the JSS and 51% for the NJSS. The enhancement is attributed mainly to thin-film evaporation sustained by capillary action in the wick and to the superior photothermal conversion of the carbon black/PVA coating, resulting in higher basin water temperatures.

Keywords: solar still; thermal evaporation; coating; interfacial material

1. Introduction

Freshwater scarcity is now ranked among the most severe long-term risks to humanity. Although approximately 71% of Earth's surface is covered by water, only 2.5% is freshwater, and barely 0.5% is in a form (rivers, lakes, accessible aquifers) that can be readily used by communities. According to UN-Water, more than two billion people already live in countries facing high water stress, and projections suggest a supply–demand gap of about 40% within a decade if current trends continue. The pressure is most acute in arid and semi-arid regions, in coastal areas with brackish groundwater, and in remote settlements that lack centralised infrastructure [1,2].

Check for updates

Academic Editor: Eugen Rusu

Published: 22 October 2026

Copyright: © 2026 by the author. Licensee MDPI, Basel, Switzerland. This article is an open access article distributed under the terms and conditions of the Creative Commons Attribution (CC BY) license.

The aim of the present work is to quantify, under identical climatic conditions, the hourly performance benefits achievable by (i) a plain jute cloth wick over a conventional basin and (ii) the same jute cloth dip-coated with carbon black nanoparticles. To this end, three geometrically identical 1.0 m^2 single-slope solar stills—referred to hereafter as CSS (conventional still), JSS (jute-wick still) and NJSS (nano-enhanced jute-wick still)—were fabricated and operated side-by-side on a clear-sky day. The contributions of this study are (a) a low-cost, dip-and-dry carbon black coating procedure that is expected to raise the solar absorptivity of the wick to about 0.93, based on values reported for carbon black-coated textiles [3], (b) a side-by-side hourly dataset that isolates the effect of the wick configuration from all other variables, and (c) a combined energy, exergy and techno-economic assessment to support practical decision-making for off-grid deployment. Research on wick-based and nano-enhanced solar stills has expanded rapidly over the last decade. The most relevant trends and representative studies are summarised below.

1.1. Natural Fibre Wick Stills

Murugavel and Srithar [4] reported a 29% yield enhancement using a cotton-wick basin in a single-basin double-slope still and emphasised the role of thin-film evaporation. Pal et al. [5] tested a multi-wick still incorporating four hydrophilic layers of jute cloth and reported a 36% gain over a conventional still under similar conditions, attributing the improvement to enlarged evaporative area and reduced thermal inertia of the saturated wick. Comparable results have been obtained with coconut coir, cotton, and luffa-sponge wicks, generally yielding 25–55% improvements depending on the geometry and operating conditions. While natural fibre wicks are inexpensive and biodegradable, their thermal absorptivity is limited, and they can suffer from gradual scaling and biofouling, motivating either chemical surface modification or active replacement protocols.

1.2. Nano-Enhanced Solar Stills

Two main approaches have emerged. The first uses metal-oxide nanoparticles (Al_2O_3, CuO, TiO_2, ZnO) dispersed in the basin water as a stable nanofluid; Kabeel et al. [6] reported a 53% gain with CuO nanofluid and Sahota and Tiwari [7] reported a 47% gain with Al_2O_3 nanoparticles. The challenges include long-term colloidal stability, scaling on absorber surfaces and the need for periodic replenishment of nanoparticles lost to the distillate or to the sludge. The second approach uses nano-coatings applied directly on the absorber surface, the wick or the basin, so the nanoparticles remain at the air–water interface where evaporation takes place and act as broadband solar absorbers. Sharshir et al. [8] reported a 73% gain using a graphene-coated absorber combined with glass cover cooling, while several recent studies on MXene, carbon nanotube, and carbon black coatings have reported gains in the range 60–100%. Carbon black is particularly attractive because of its very broad absorption spectrum, its very low cost, and its compatibility with simple aqueous deposition methods. To the best of the author's knowledge, no prior study has reported a direct side-by-side hourly comparison of plain jute and carbon black-coated jute wicks under identical climatic conditions in a single-slope solar still, which is the contribution of the present work.

2. Materials and Methods

2.1. Experimental Setup

Three geometrically identical single-slope solar stills (CSS, JSS, NJSS) were fabricated locally and tested in parallel under clear-sky conditions. Each still had an effective basin area of 1.0 m^2 (1.0 m × 1.0 m), a basin made of 1.5 mm galvanised steel with a matte-black absorber coating, a 4 mm transparent glass cover inclined at 24° (approximately equal to the

site latitude), and 30 mm of glass wool insulation on the side walls and base. A V-shaped stainless-steel condensate channel was fitted under the lower edge of the cover, feeding a graduated collector. A float-controlled feed water inlet kept the water depth at 20 mm in all three stills throughout the experiment. The only difference between the three units was the basin–absorber configuration: CSS used the bare black-painted basin (plain absorber); JSS used a plain jute cloth (280 g/m^2) placed over the basin so that capillary action maintained a thin film of saline water on the wick; and NJSS used the same jute cloth that had been dip-coated with carbon black nanoparticles. The saline feed water was prepared to a total dissolved solids concentration of approximately 4500 ppm (NaCl-equivalent), which is representative of moderately brackish groundwater. A schematic of the experimental arrangement is given in Figure 1, showing (a) the cross-section of the single-slope still and (b) the three units with their basin configurations and instrumentation.

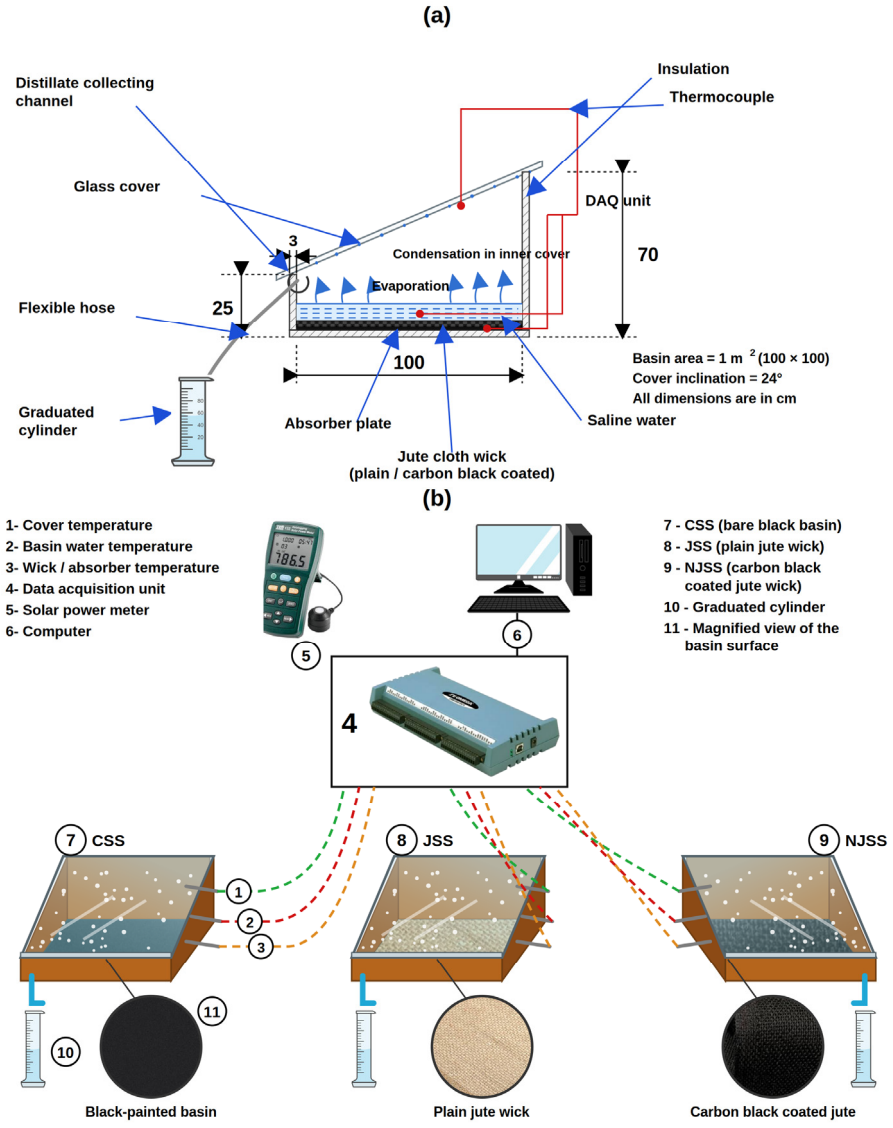


Figure 1. Schematic of the experimental setup: (**a**) cross-sectional view of the single-slope solar still (dimensions in cm) and (**b**) the three stills tested side-by-side—CSS (bare black-painted basin), JSS (plain jute wick) and NJSS (carbon black-coated jute wick)—with the thermocouple locations, solar power metre, data acquisition unit and graduated cylinders.

2.2. Geometric and Operating Parameters

The geometric and operating parameters for the solar still (3 configurations) are presented in Table 1.

Table 1. Geometric and operating parameters.

Parameter	Value
Effective basin area	1.0 m^2 (1.0 m × 1.0 m)
Glass cover	4 mm thickness; transmissivity τ = 0.87
Cover inclination angle	24° (site latitude)
Basin material	1.5 mm galvanised steel, matte-black-coated
Insulation (walls and base)	30 mm glass wool, k = 0.04 W/m·K
Feed water (TDS)	4500 ppm
Water depth (regulated)	20 mm, float-controlled
Test window	08:00–18:00 local time, one representative clear-sky day

2.3. Wick Preparation Methodology

Plain jute cloth (areal density = 280 g/m^2) was cut to the basin dimensions (1.0 × 1.0 m). For the nano-coated wick of the NJSS, the following dip-and-dry deposition procedure was used. A homogeneous aqueous suspension containing 1.0 wt% carbon black powder (primary particle size = 30 nm, manufacturer-reported) and 0.2 wt% polyvinyl alcohol (PVA) as a film-forming binder was prepared and ultrasonicated for 20 min to break agglomeration. The jute cloth was fully immersed in this bath for 30 min, with gentle agitation every five minutes to ensure complete saturation. The wet cloth was then drained, hung to air-dry for 12 h at ambient temperature, and finally cured in a convection oven at 60 °C for 2 h to lock in the binder. After curing, the cloth was rinsed under gentle running water to remove any loose particles and then weighed; the gravimetric mass loading of carbon black was estimated at 12 g/m^2 of jute surface. Direct visual inspection and a wash-fastness test (five repeated rinse cycles) confirmed that the coating was visually uniform across the cloth and was not removed by rinsing and handling.

Characterisation of the coated wick in this study was limited to the gravimetric carbon black loading, visual inspection and the wash-fastness test. The nanoscale size of the carbon black is therefore based on the manufacturer's specification of the primary particle size (30 nm). The solar absorption of 94–98.6% has been reported for carbon black-coated textiles [3]. No quantitative value is available for the plain jute used here, whose light-brown colour is expected to give a noticeably lower absorptivity; the comparison between the two wicks is therefore qualitative. These values are used only to interpret the thermal results, and the actual absorptivity of the present wicks may differ. SEM imaging of the jute before and after coating, to assess the carbon black distribution, and spectrophotometric measurement of the wick absorptivity are planned as future work.

2.4. Instrumentation and Data Acquisition

All measurements were logged through a 24-channel data acquisition (DAQ) unit at a sampling interval of 1 s and subsequently averaged over 1 min and 1 h intervals as required. Global solar irradiance on the horizontal plane was measured with a thermopile pyranometer; ambient air temperature, relative humidity, and wind speed were measured with a co-located weather station. Temperatures of the basin water, glass cover (inner surface), wick surface, and ambient air were measured with calibrated K-type thermocouples installed at three locations per surface and averaged. The hourly distillate yield was collected in graduated cylinders (1000 mL ± 10 mL). All sensors were recalibrated against reference standards on the day prior to each experiment. The accuracies of the instruments were ±0.5 °C for the calibrated K-type thermocouples, ±2% of reading for

the pyranometer and ±10 mL for the graduated cylinders; the resulting uncertainties are evaluated in Section 2.6.

2.5. Performance Indicators

The thermal performance of each still was evaluated on both first-law (energy) and second-law (exergy) bases. The hourly distillate productivity is given as [9],

$$\dot{m}_{ew} = \frac{Q_{ew}}{h_{fg}\, A_b} \tag{1}$$

where $\dot{m}_{ew}$ is the hourly mass of distillate per unit basin area (kg/m^2·h), Q_{ew} is the evaporative heat-transfer rate (W), h_{fg} is the latent heat of vaporisation of water (J/kg) evaluated at the average basin temperature, and A_b is the basin area (m^2). The hourly thermal (energy) efficiency is

$$\eta_{en} = \frac{\dot{m}_{ew}\, h_{fg}}{I_g\, A_b} \tag{2}$$

where I_g is the global solar irradiance (W/m^2). The daily thermal efficiency is obtained by integration over the operating window,

$$\eta_{en,daily} = \frac{\sum \dot{m}_{ew}\, h_{fg}}{\sum I_g\, A_b} \tag{3}$$

Exergy efficiency was evaluated using the Petela framework for solar radiation. The useful exergy associated with evaporation and the exergy of the solar flux on the basin area is given as [10],

$$Ex_{evap} = \dot{m}_{ew}\, h_{fg} \left(1 - \frac{T_a}{T_w}\right) \tag{4}$$

$$Ex_{solar} = I_g\, A_b \left[1 - \frac{4}{3}\left(\frac{T_a}{T_s}\right) + \frac{1}{3}\left(\frac{T_a}{T_s}\right)^4\right] \tag{5}$$

with T_a and T_w the ambient and basin water temperatures expressed in K and T_s = 6000 K the apparent black-body temperature of the sun. The hourly Petela exergy efficiency follows directly as

$$\eta_{ex} = \frac{Ex_{evap}}{Ex_{solar}} \tag{6}$$

2.6. Uncertainty Analysis

The uncertainties in the measured and derived quantities were estimated using the root-sum-square method of Kline and McClintock [11]. For a result R that depends on n independent measured variables x_i, each with uncertainty w_xi, the uncertainty of R is given by Equation (7):

$$w_R = \left[\sum_{i=1}^{n}\left(\frac{\partial R}{\partial x_i}\, w_{x_i}\right)^2\right]^{\frac{1}{2}} \tag{7}$$

The hourly distillate yield carries the cylinder uncertainty of ±10 mL/m^2. Since the daily yield Y_d is the sum of 11 hourly readings, its uncertainty is $\sqrt{11} \times 10$ mL = ±0.033 L/m^2. The latent heat and basin area contribute negligibly, so the relative uncertainty of the daily energy efficiency follows from Equation (8):

https://doi.org/10.3390/engproc2026152024

$$\frac{w_{\eta_{en}}}{\eta_{en}} = \sqrt{\left(\frac{w_{Y_d}}{Y_d}\right)^2 + \left(\frac{w_{I_g}}{I_g}\right)^2} \tag{8}$$

The exergy efficiency additionally depends on the Carnot factor $\varphi = 1 - T_a/T_w$ in Equation (4). The factor involving the sun temperature in Equation (5) is insensitive to T_a because $T_a \ll T_s$. The uncertainty of φ is given by Equation (9), and the relative uncertainty of the exergy efficiency by Equation (10):

$$w_\varphi = \sqrt{\left(\frac{w_{T_a}}{T_w}\right)^2 + \left(\frac{T_a\, w_{T_w}}{{T_w}^2}\right)^2} \tag{9}$$

$$\frac{w_{\eta_{ex}}}{\eta_{ex}} = \sqrt{\left(\frac{w_{\eta_{en}}}{\eta_{en}}\right)^2 + \left(\frac{w_\varphi}{\varphi}\right)^2} \tag{10}$$

Applying Equations (7)–(10) with the instrument accuracies listed in Section 2.4, the uncertainty of the daily yield is ±0.033 L/m^2, corresponding to ±1.6%, ±1.1% and ±0.9% for the CSS, JSS and NJSS, respectively. The daily energy efficiency is uncertain by ±0.9, ±1.0 and ±1.1 percentage points, and the daily exergy efficiency by ±0.11, ±0.14 and ±0.17 percentage points. The measured temperatures are uncertain by ±0.5 °C and the solar irradiance by ±2% of reading. These uncertainties are shown as error bars in Figures 2 and 3.

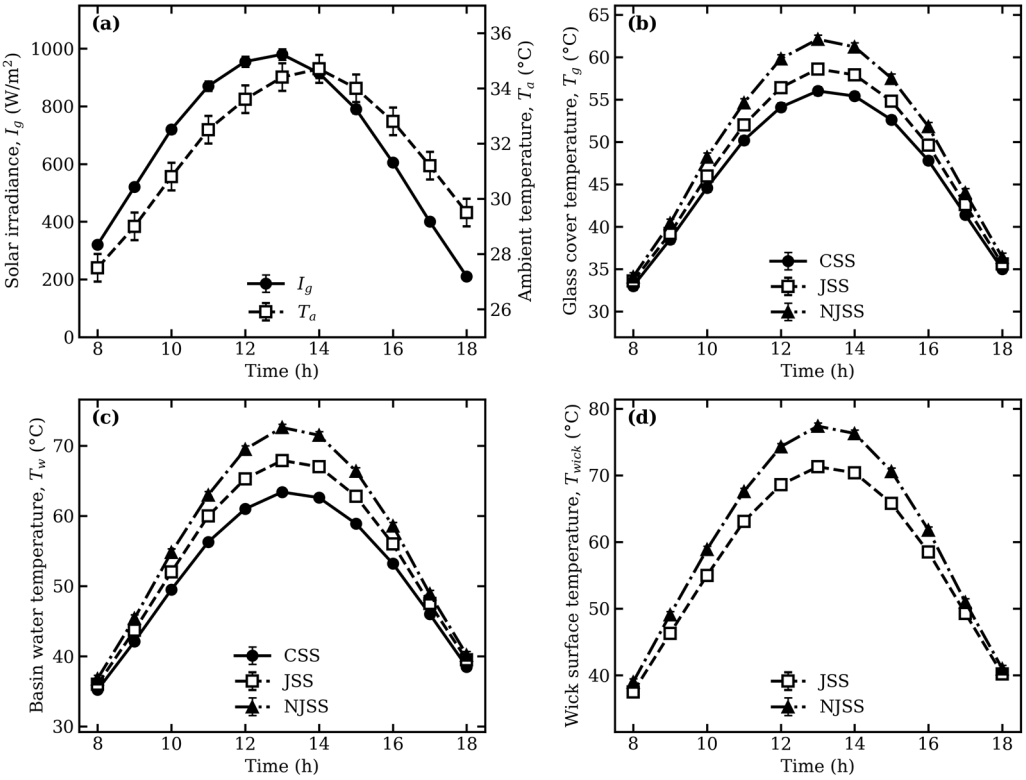


Figure 2. Hourly thermal behaviour of the CSS, JSS and NJSS stills under clear-sky conditions: (**a**) solar irradiance and ambient temperature; (**b**) glass cover temperature; (**c**) basin water temperature; (**d**) wick surface temperature.

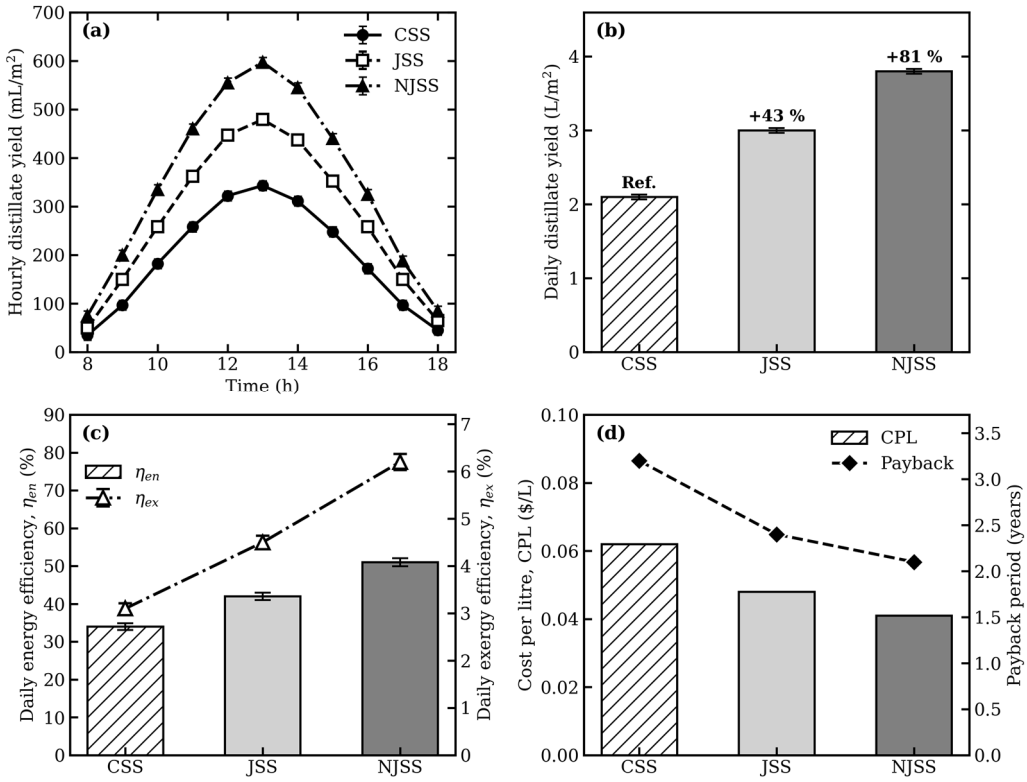


Figure 3. Performance and techno-economic comparison of the three stills: (**a**) hourly distillate yield; (**b**) daily yield with gain over CSS; (**c**) daily energy and exergy efficiency; (**d**) cost per litre and payback period.

3. Results and Discussion

3.1. Solar Radiation and Ambient Temperature

The results presented in this study were obtained on a single clear-sky test day, which was characterised by a peak global solar irradiance of Ig = 980 W/m^2 at 13:00 and a daily integrated solar input of approximately 7.29 kWh/m^2. The ambient temperature rose smoothly from 27.5 °C at 08:00 to a peak of 34.7 °C at 14:00, then declined to 29.5 °C by 18:00 h (Figure 2a). Because all three stills were exposed simultaneously to the same incident radiation and ambient conditions, any observed difference in their thermal and productivity behaviour can be attributed unambiguously to the wick configuration. Before the test, all three stills were supplied with the same feed water (4500 ppm) at the same regulated depth of 20 mm, and data recording started simultaneously at 08:00, so that the initial conditions were also identical.

3.2. Hourly Condensing Cover Temperature

The temperature of the inner surface of the glass cover, T_g, is the most important condensation parameter—it sets the driving temperature difference ($T_w - T_g$) that controls the evaporation–condensation cycle. As shown in Figure 2b, all three covers followed the same heating profile shape, peaking around 13:00, but the absolute values differed by the configuration. The peak T_g was 56.0, 58.6, and 62.1 °C for the CSS, JSS, and NJSS, respectively. The 6 °C warmer cover of the NJSS confirms that more vapour reaches the cover and condenses there (releasing latent heat that raises the cover temperature). Despite the warmer cover, the temperature gap ($T_w - T_g$) was preserved in all configurations, ensuring efficient condensation throughout the day.

https://doi.org/10.3390/engproc2026152024

3.3. Hourly Basin Water Temperature

The temperature of the basin water, T_w, drives the evaporative process: higher T_w produces a higher vapour pressure at the liquid–air interface and thus a higher mass-transfer rate. As reported in Figure 2c, T_w in the NJSS exceeded that of the CSS by 7–10 °C throughout the day and peaked at 72.6 °C against 63.4 °C for CSS—a 9 °C improvement. The JSS lay in between, peaking at 67.9 °C. The mechanism is twofold: the thin capillary film over the wick has a much smaller thermal mass than the deeper basin water, so it heats up faster, and the higher absorptivity of the nano-coated jute (about 0.93, a representative value for carbon black-coated textiles [3]) captures a larger fraction of incident solar energy directly at the air–water interface.

3.4. Hourly Wick Surface Temperature

The wick surface temperature T_{wick} measured for the JSS and NJSS is the most direct indicator of the photothermal interface activity (Figure 2d). The nano-coated wick of the NJSS reached 77.4 °C at 13:00 against 71.3 °C for the plain jute under the same conditions—a 6 °C difference at peak. Because the wick is thin and largely composed of fibres with limited thermal mass, this temperature responds rapidly to changes in solar input. The local overheating of the wick by 5 °C above the bulk basin water in the NJSS is consistent with the localised photothermal evaporation paradigm: the absorbed solar energy is dissipated mainly at the air–water interface on the wick fibres, producing very efficient vapour generation while keeping the deeper water cooler.

3.5. Hourly Distillate Yield Collected

The hourly distillate yield is the primary product of the still and the most informative measure of overall performance. As reported in Figure 3a, NJSS consistently produced the highest yield at every hour, JSS came second, and CSS the lowest, in line with their thermal behaviour discussed in Sections 3.2–3.4. The peak hourly yields at 13:00 were 343, 479 and 597 mL/m^2 for CSS, JSS and NJSS, respectively. Importantly, both modified stills retained significant production in the late afternoon (16:00–18:00), where they produced 220–260 mL/m^2 compared with only 130 mL/m^2 for the CSS—evidence of the modest thermal storage role of the wet fibrous mass.

3.6. Analysis of Energy Efficiency

Applying Equation (2) hour by hour gives the instantaneous thermal efficiency of each still as a function of time. All three configurations followed a bell-shaped daily profile, peaking near 13:00 h, but NJSS dominated at every hour, and the gap widened with irradiance. Integrating over the full operating window using Equation (3) yielded a daily thermal efficiency of 34%, 42% and 51% for CSS, JSS and NJSS, respectively. Because the jute cloth lies flat on the basin, the projected evaporation area remains 1.0 m^2 in all three stills; the microscopic fibre texture may increase the wetted surface locally, but this contribution was not quantified in the present study and is expected to be secondary. Instead, capillary action in the jute sustains a thin saline film of low thermal mass at the absorbing surface, so that (i) the absorbed solar energy is concentrated in a thin, rapidly heated layer at the air–water interface where evaporation takes place, (ii) the higher absorptivity of the carbon black-coated wick (about 0.93, a representative value for carbon black-coated textiles [3], compared with the lower absorptivity of light-brown plain jute) raises the interface temperature further, and (iii) the small thermal inertia of the film produces a faster response to changes in incident radiation (Figure 3c).

https://doi.org/10.3390/engproc2026152024

3.7. Analysis of Exergy Efficiency

The exergy analysis using Equations (4)–(6) provides a stricter, second-law assessment. The exergy efficiency of solar stills is always much lower than the energy efficiency because the process operates at a small temperature lift between the basin water and ambient air, so the Carnot factor ($1 - T_a/T_w$) is modest (Figure 3c). The daily-averaged Petela exergy efficiencies obtained here were 3.1%, 4.5% and 6.2% for CSS, JSS and NJSS, respectively. Doubling the exergy efficiency between CSS and NJSS is significant: it indicates that the wick coating not only increases the quantity of distillate produced (energy gain) but also raises the quality of the heat used, by pushing the basin water to a higher temperature and therefore a higher Carnot factor.

3.8. Economic Analysis

A simple techno-economic comparison was carried out using the capital recovery factor (*CRF*) and sinking fund factor (*SFF*) method commonly used in solar still studies (Figure 3d). The annualised fixed cost (*AFC*), the cost per litre (*CPL*) of distillate and the payback period (*PP*) are obtained using the following equations, with the baseline inputs summarised in Table 2.

Table 2. Baseline inputs and results of the techno-economic analysis (Equations (11)–(15)).

Parameter	CSS	JSS	NJSS
Interest rate, i (%)	10	10	10
Service life, n (years)	10	10	10
CRF/SFF	0.1627/0.0627	0.1627/0.0627	0.1627/0.0627
Capital cost, P ($)	225	245	270
Salvage value, S = 0.2P ($)	45	49	54
Annual maintenance cost, AMC = 0.15·CRF·P ($/year)	5.49	5.98	6.59
Operating days per year	300	300	300
Daily yield (L/m^2)	2.10	3.00	3.80
Annual yield, Y_{annual} (L/year)	630	900	1140
Annualised fixed cost, AFC ($/year)	39.29	42.78	47.14
Selling price of distillate, SP ($/L)	0.12	0.12	0.12
Cost per litre, CPL ($/L)	0.062	0.048	0.041
Payback period, PP (years)	3.2	2.4	2.1

The capital recovery factor is defined by Equation (11):

$$CRF = \frac{i(1+i)^n}{(1+i)^n - 1} \tag{11}$$

The sinking fund factor is given by Equation (12):

$$SFF = \frac{i}{(1+i)^n - 1} \tag{12}$$

The annualised fixed cost is obtained from Equation (13):

$$AFC = CRF \cdot P - SFF \cdot S + AMC \tag{13}$$

The cost per litre of distillate is given by Equation (14):

$$CPL = \frac{AFC}{Y_{annual}} \tag{14}$$

https://doi.org/10.3390/engproc2026152024

The simple payback period is estimated from Equation (15), in which the net annual income is the revenue from the sale of distillate less the annual maintenance cost:

$$PP = \frac{P}{Y_{annual} \cdot SP - AMC} \quad (15)$$

In Equations (11)–(15), i is the annual interest rate, n is the service life of the still (years), P is the initial capital cost, S is the salvage value, AMC is the annual maintenance cost, Y_{annual} is the annual distillate yield and SP is the selling price of distillate. The baseline inputs are listed in Table 2. An interest rate of 10% and a service life of 10 years were assumed for all three stills, giving CRF = 0.1627 and SFF = 0.0627. The capital cost of the 1.0 m^2 CSS was taken as \$225; the incremental costs of the JSS (\$245) and NJSS (\$270) correspond to the plain jute wick and to the jute wick with the carbon black/PVA dip-coating, respectively. The salvage value was taken as 20% of the capital cost, and the annual maintenance cost as 15% of the annualised capital cost (CRF·P), i.e., \$5.49, \$5.98 and \$6.59 per year for the CSS, JSS and NJSS, covering glass cover cleaning and sealant renewal; wick replacement is treated separately below. The annual yield was obtained from the measured daily yields assuming 300 clear-sky operating days per year, and a selling price of 0.12 \$/L was used for the payback period calculation.

With these inputs, the cost per litre of distillate was reduced by 34% (from 0.062 \$/L for the CSS to 0.048 \$/L for the JSS and 0.041 \$/L for the NJSS) and the payback period dropped from 3.2 to 2.4 and 2.1 years, respectively (Table 2 and Figure 3d). Because the higher capital cost of the modified stills is outweighed by their larger annual yield, the NJSS remains the most economical configuration despite being the most expensive to build.

The long-term durability of the jute wick was not assessed in this study; the five-cycle wash test (Section 2.3) confirms only short-term coating adhesion. Because natural fibres are prone to biodegradation, mildew and salt scaling in warm brackish water, periodic wick replacement is expected in field operation. Its effect on the economics was therefore evaluated by adding the wick replacement cost (\$3 for plain jute and \$5 for carbon black-coated jute per 1 m^2 wick) as an annual cost for replacement intervals of 12, 6 and 3 months (Table 3). Frequent replacement increases the NJSS cost per litre from 0.041 to 0.059 \$/L and its payback period from 2.1 to 2.5 years under quarterly replacement. Both values nevertheless remain below those of the CSS (0.062 \$/L and 3.2 years), indicating that the economic benefit of the nano-coated wick persists even with short wick lifetimes.

Table 3. Sensitivity of cost per litre and payback period to the wick replacement interval (CSS: 0.062 \$/L, 3.2 years, no wick).

Replacement Interval	JSS CPL (\$/L)	JSS PP (years)	NJSS CPL (\$/L)	NJSS PP (years)
No replacement	0.048	2.4	0.041	2.1
12 months	0.051	2.5	0.046	2.2
6 months	0.054	2.6	0.050	2.3
3 months	0.061	2.7	0.059	2.5

4. Conclusions

A side-by-side experimental comparison of a conventional single-slope solar still (CSS), a jute-wick still (JSS) and a nano-enhanced jute-wick still (NJSS) was carried out under identical conditions on a representative clear-sky day. The principal conclusions are:

- Daily distillate yield rose from 2.10 L/m^2 (CSS) to 3.00 L/m^2 (JSS) and 3.80 L/m^2 (NJSS), corresponding to gains of 43% and 81%, respectively.
- Basin water temperature at peak hour was raised by up to 9 °C and wick surface temperature by up to 14 °C with the carbon black/PVA-coated jute, consistent with a photothermal localization mechanism.
- Daily-integrated thermal efficiency improved from 34% (CSS) to 42% (JSS) and 51% (NJSS); the daily Petela exergy efficiency doubled from 3.1% to 6.2%.
- The cost per litre of distillate was reduced by 34% (from 0.062 $/L to 0.041 $/L) and the payback period dropped from 3.2 to 2.1 years.
- Carbon black-coated jute is a simple, low-cost photothermal wick suitable for off-grid freshwater production, and its economic advantage over the conventional still is retained even if the wick is replaced every three months. Its long-term operational lifespan was not measured here. Because the results were obtained on a single test day and the absorptivity values were taken from the literature, they should be regarded as a comparative demonstration. Future work will include repeated tests over multiple days and seasons, SEM characterisation of the coated fibres, spectrophotometric measurement of the wick absorptivity, a jute + PVA control wick, and durability tests under prolonged brackish-water exposure, together with optimum nanoparticle loading and integration with phase-change materials.

Funding: This research received no external funding.

Institutional Review Board Statement: Not applicable.

Informed Consent Statement: Not applicable.

Data Availability Statement: Dataset available on request from the author.

Acknowledgments: During the revision of this manuscript, the author used Claude (Anthropic, Opus 5, September 2026) for language editing. The author has reviewed and edited the output and takes full responsibility for the content of this publication.

Conflicts of Interest: The author declares no conflicts of interest.

References

1. UN-Water. *Summary Progress Update 2024—SDG 6 on Water and Sanitation*; UN-Water: Geneva, Switzerland, 2024.
2. Tiwari, G.N.; Singh, H.N.; Tripathi, R. Present status of solar distillation. *Sol. Energy* **2003**, *75*, 367–373. [CrossRef]
3. Saeed, H.A.M.; Kazimoto, V.V.; Xu, W.; Yang, H. The Application of Textile Materials in Interfacial Solar Steam Generation for Water Purification and Desalination. *Polymers* **2024**, *16*, 793. [CrossRef] [PubMed]
4. Murugavel, K.K.; Srithar, K. Performance study on basin-type double-slope solar still with different wick materials and minimum mass of water. *Renew. Energy* **2011**, *36*, 612–620. [CrossRef]
5. Pal, P.; Yadav, P.; Dev, R.; Singh, D. Performance analysis of modified basin type double-slope multi-wick solar still. *Desalination* **2017**, *422*, 68–82. [CrossRef]
6. Kabeel, A.E.; Omara, Z.M.; Essa, F.A. Improving the performance of solar still by using nanofluids and providing vacuum. *Energy Convers. Manag.* **2014**, *86*, 268–274. [CrossRef]
7. Sahota, L.; Tiwari, G.N. Effect of nanofluids on the performance of passive double slope solar still: A comparative study using characteristic curve. *Desalination* **2016**, *388*, 9–21. [CrossRef]
8. Sharshir, S.W.; Peng, G.; Wu, L.; Yang, N.; Essa, F.A.; Elsheikh, A.H.; Show, P.L.; Kabeel, A.E. The effects of flake graphite nanoparticles, phase change material, and film cooling on the solar still performance. *Appl. Energy* **2017**, *191*, 358–366. [CrossRef]
9. Dunkle, R.V. Solar water distillation: The roof type still and a multiple effect diffusion still. In Proceedings of the International Heat Transfer Conference, Boulder, CO, USA, 28 August–1 September 1961; Part V, Paper 108, pp. 895–902.

10. Petela, R. Exergy of heat radiation. *J. Heat Transf.* **1964**, *86*, 187–192. [CrossRef]
11. Kline, S.J.; McClintock, F.A. Describing uncertainties in single-sample experiments. *Mech. Eng.* **1953**, *75*, 3–8.

Disclaimer/Publisher's Note: The statements, opinions and data contained in all publications are solely those of the individual author(s) and contributor(s) and not of MDPI and/or the editor(s). MDPI and/or the editor(s) disclaim responsibility for any injury to people or property resulting from any ideas, methods, instructions or products referred to in the content.